

NORDITA 98/79
 LTH – 449
 February 1, 2008

Two heavy-light mesons on a lattice

UKQCD Collaboration

C. Michael^{1,2} and P. Pennanen^{3,4}

¹*Theoretical Physics Division, Dept. of Math. Sciences, University of Liverpool, Liverpool, UK.*

³*Nordita, Blegdamsvej 17, DK-2100 Copenhagen Ø, Denmark*

Abstract

The potential between two heavy-light mesons as a function of the heavy quark separation is calculated in quenched SU(3) lattice QCD. We study the case of heavy-light mesons with a static heavy quark and light quarks of mass close to the strange quark mass. We explore the case of light quarks with the same and with different flavours, classified according to the light quark isospin. We evaluate the appropriate light quark exchange contributions and explore the spin-dependence of the interaction. Comparison is made with meson exchange.

PACS numbers: 13.75.Lb, 11.15.Ha, 12.38.Gc, 25.80.-e

1 Introduction

The progress in lattice QCD has so far been mainly restricted to systems of three quarks or less. However, there is also considerable interest in obtaining

²E-mail: cmi@liv.ac.uk

⁴petrus@hip.fi

predictions from first principles for multi-quark systems which can be decomposed into more than one colour singlet. In addition to the complicated cases of nuclei, simple multi-quark systems have been proposed to exist as bound states [1, 2, 3]. Four quarks forming colour singlets or as bound states of two mesons are candidates for particles lying close to meson-antimeson threshold, such as $a_0(980)$, $f_0(980)$ ($K\bar{K}$), $f_0(1500)$, $f_2(1500)$ ($\omega\omega$, $\rho\rho$), $f_J(1710)$ ($K^*\bar{K}^*$), $\psi(4040)$ ($D^*\bar{D}^*$), $\Upsilon(10580)$ ($B^*\bar{B}^*$) [4].

Systems with heavy quarks should be more easily bound provided the potential is attractive, since the repulsive kinetic energy of the quarks is smaller, while the attractive two-body potential remains the same. In so-called deuson models [5] the long-range potential between two mesons comes from one-pion exchange, suggesting that meson-meson systems are significantly less bound than meson-antimeson systems. Other models used for four-quark systems include string-flip potential models (see Ref. [6] for a review), bag models [2], and a model-independent approach [7]. Four-quark states with two heavy quarks have been predicted to be stable [8]. Most models give stability for systems where the heavy quarks have the b mass, but long range forces might push the required heavy-to-light mass ratio down so that $cc\bar{q}\bar{q}$ states would be bound as well.

Static four-quark systems [9] (and references therein) have been previously studied for a set of geometries representative of the general case and a model was constructed that reproduces one hundred ground and excited state energies with four independent parameters [10]. The model is based on ground- and excited state two-body potentials and multi-quark interaction terms. The results show that, in a two-body potential approach to understanding multi-quark interaction, the effect from gluonic excitations is needed, and their relative contribution to the binding becomes more important (even dominant) at larger distances. Flux distributions corresponding to the binding energies of four static quarks are studied in Ref. [11].

Moving on to more realistic systems, we now study in detail the potential between two heavy-light mesons. Exploratory studies of two-meson systems have been made for the cross diagram only (Fig. 1 below) for SU(3) colour [12] and for both diagrams in Refs. [13], [14] for SU(2), SU(3) colour respectively.

We take the mass of one quark in each meson to be heavy – the prototype being the B meson. This is in the spirit of the heavy quark effective theory

approach which describes the leading term (the static limit) and the corrections of higher orders in $1/m_Q$. In the static approximation for the heavy quarks, the pseudoscalar B meson and the vector B^* meson will be degenerate – whereas they are split by 46 MeV experimentally. Since we shall often have occasion to treat this degenerate set together we describe this case as the \mathcal{B} meson. In analogy to the Born-Oppenheimer approximation, we will then discuss the potential energy between static \mathcal{B} mesons.

For the light quarks, we use the full relativistic description with a fermion action which is the $O(a^2)$ improved Sheikholeslami-Wohlert clover action with a tadpole-improved coefficient. We should in principle evaluate the interaction for several light quarks masses and then extrapolate to the physical values. In this preliminary study, we fix the light quark mass at around the strange mass. We do however consider the case of two flavours of quark – so allowing a discussion of different isospin states. The main reason why this study is difficult to perform on a lattice is that the light quark propagators are needed from many different sources. To achieve this we make use of the technique of evaluating the light quark propagators as stochastic estimates [15] using maximal variance reduction introduced in Ref. [16].

Quenched lattices are used with $SU(3)$ colour and static heavy quarks with light quarks of approximately the strange quark mass. Preliminary versions of this work have appeared [21]. Here the isospin and spin degrees of freedom are discussed in detail. We compare our results for small separation R with the known spectrum of baryons with one heavy quark (Λ_b and Σ_b). This will enable us to discover if a heavy diquark is a good description. Note that this link which we find to baryons at small separation R cannot be explored using $SU(2)$ of colour. We also compare our results with the expectations of meson exchange. We find that at larger R , this is a useful guide to the interaction strength and, for pion exchange, we are able to make a quantitative comparison. We comment on the agreement with other models, one of them being the potential model for static systems applied in this more dynamic case [19].

2 $\mathcal{B}\mathcal{B}$ interactions in the static approximation

We take the mass of one quark in each meson to be very heavy – the prototype being the B meson. The static limit is then the leading term in the heavy quark effective theory for a heavy quark of zero velocity and there will be corrections of higher orders in $1/m_Q$ where m_Q is the heavy quark mass. In the limit of a static heavy quark, the heavy quark spin is uncoupled since the relevant magnetic moment vanishes which implies that the pseudoscalar B meson and the vector B^* meson will be degenerate. This is a reasonable approximation since they are split by 46 MeV experimentally, which is less than 1% of the mass of the mesons. Since we shall often have occasion to treat these two mesonic states as if they were degenerate, we describe them collectively as the \mathcal{B} meson. Because of the insensitivity to the heavy quark spin, it is then appropriate to classify these degenerate \mathcal{B} meson states by the light quark spin: so there are only two independent spin states. The system of two heavy-light mesons at spatial separation R will be referred to as the $\mathcal{B}\mathcal{B}$ system. With both heavy-light mesons static, this $\mathcal{B}\mathcal{B}$ system is described by the spin states of the two light quarks in the two mesons. Thus there are four possible states and we need to classify the interaction in terms of these spin states.

This situation is very similar to that of the hydrogen molecule in the Born-Oppenheimer approximation – with, however, the additional possibility that the two ‘electrons’ can have different properties. Another similarity is with the potential between quarks which has a central component and then scalar and tensor spin-dependent contributions.

Each \mathcal{B} meson will have a light quark flavour assignment. For the $\mathcal{B}\mathcal{B}$ system, it will be appropriate to classify these states according to their symmetry under interchange of the light quark flavours. For identical flavours (eg. ss or uu), we have symmetry under interchange, whereas for non-identical flavours (eg. su or du), we may have either symmetry or antisymmetry. For two light quarks, it is convenient to classify the states according to isospin as $I = 1$ (with uu , $ud + du$ and dd) or $I = 0$ (with $ud - du$).

We now present a discussion of the possible states of two \mathcal{B} mesons. As a guide we show in Table 1 the states for the case of an S-wave $\mathcal{B}\mathcal{B}$ system in the limit of static \mathcal{B} mesons. We must have overall symmetry of the wavefunction under interchange and, assuming symmetry for spatial interchange,

the flavour, total light quark spin (S_q) and total heavy quark spin (S_b) must be combined to achieve this. Thus in the limit of an isotropic spatial wavefunction, there will be the four different ground state levels of the $\mathcal{B}\mathcal{B}$ system as shown in Table 1 since the three states with different J^P but the same light quark isospin I_q and spin S_q will be degenerate in the static limit. We will label these states by I_q , S_q for subsequent discussion. We also show which physical B and B^* mesons couple to these states. This table can also be extended to $L \neq 0$ levels. In particular, we shall later see that a tensor interaction may be present, in which case the $S_q = 1$ ground states will show an admixture of $L = 0$ and of $L = 2$.

Table 1: Allowed $\mathcal{B}\mathcal{B}$ states with $L = 0$

I_q	S_q	S_b	J^P	BB	BB*	B^*B^*
1	1	1	0^+	Yes		Yes
1	1	1	1^+		Yes	
1	1	1	2^+			Yes
1	0	0	0^+	Yes		Yes
0	1	0	1^+		Yes	Yes
0	0	1	1^+		Yes	Yes

When $R = 0$, the situation is special since the colour of the two static quarks can be combined. This net colour can be in a anti-triplet (antisymmetric under particle exchange) or a sextet (symmetric under particle exchange). The former case is just that of the static baryons. This equivalence implies that the $I_q = 1$, $S_q = 1$ state will have the same light quark structure as the Σ_b baryon, while the $I_q = 0$, $S_q = 0$ state will be as the Λ_b baryon. The other two allowed $\mathcal{B}\mathcal{B}$ states at $R = 0$ correspond to a static sextet source.

In a Born-Oppenheimer treatment of the $\mathcal{B}\mathcal{B}$ system, we will need to consider the potential energy for the \mathcal{B} mesons at rest at separation R . This $\mathcal{B}\mathcal{B}$ system can be classified under rotations about the separation axis, here taken as the z axis, and under interchange of the two mesons. Taking the z axis to quantise the light quark spin, we have states with $J_z = \pm 1$, namely $| + + \rangle$, $| - - \rangle$ and with $J_z = 0$, namely $| + - \rangle \pm | - + \rangle$. Since J_z is conserved, we can discuss the interaction energy in terms of a triplet state E_T corresponding to the $J_z = \pm 1$ cases, and then the $J_z = 0$ sector can be described by a

singlet state with energy E_S between initial and final states ($|+-\rangle - |--\rangle$) and by another triplet state E'_T for initial and final states ($|+-\rangle + |--\rangle$). These three energies can be related to a more conventional treatment using a central, spin-dependent and tensor potential. We shall instead mainly focus on the singlet, E_S , and triplet averaged over orientations, $(2E_T + E'_T)/3$. Since the heavy quark spin does not interact, the symmetric and antisymmetric combinations constructed from the heavy quark spin will allow any overall symmetry under interchange for the overall spin assignment.

In our actual numerical calculation, we use a relativistic treatment of the light quark spin but in the context of a static heavy quark with Dirac propagator structure $(1 + \gamma_4)$. This enables us to simplify the Dirac γ -matrix algebra between initial and final B mesons (created by $\bar{q}\gamma_5 b$) and B^* mesons (created by $\bar{q}\gamma_i b$). This approach also leads to three independent observables which we determine as

$$\begin{aligned} C_I &= ((++) + (--)).((++) + (--)) \\ C_s(z) &= ((++) - (--)).((++) - (--)) \\ C_s(x) = C_s(y) &= (+-).(-+) + (-+).(+-) \end{aligned}$$

with notation (13).(24) for $B_1B_2 \rightarrow B_3B_4$ with the sign of the light quark spin (S_{1z} , etc) given.

In practice the observable given above by $C_s(z)$ is also evaluated with the spatial separation R in x and y directions which gives an equivalent method to obtain $C_s(x)$ and $C_s(y)$. By symmetry, the latter two observables are equal on average. Note that the $\text{BB} \rightarrow \text{BB}$ correlation is given by C_I , whereas $\text{BB}^* \rightarrow \text{B}^*\text{B}$ is given by C_s .

It is not sufficient just to look at processes such as $BB \rightarrow BB$ since, in the heavy quark limit, there will also be other channels such as $BB \rightarrow B^*B^*$ which are coupled. We then analyse the matrix of correlations between all such channels and find the basis that diagonalises it. This leads to certain linear combinations of correlations which describe these diagonal elements. This explicit fermionic approach must reproduce the conclusions reached above by using the heavy quark limit. The relationship between these approaches is that, at large t ,

$$C_I + C_s(z) \rightarrow e^{-E_T t} \quad (1)$$

$$C_I - C_s(z) - C_s(x) - C_s(y) \rightarrow e^{-E_S t} \quad (2)$$

$$C_I - C_s(z) + C_s(x) + C_s(y) \rightarrow e^{-E'_S t} \quad (3)$$

It turns out that the same combinations (those given in the above equations) occur for both the case of symmetry under exchange of initial particles and for the case of antisymmetry. This can be understood in the heavy quark effective theory, as discussed above, since the combinations are in terms of the light quarks spins, leaving the heavy quark spins to be combined either in symmetric or antisymmetric states.

The structure of the correlations to be evaluated, in terms of the light quark propagator G and the gauge product for the static line in the negative-going t -direction of U is then

$$C_I(t) = \langle G_{ii}^{ba}(0, 0; 0, t) U^{ab}(0) G_{kk}^{dc}(e_z R, 0; e_z R, t) U^{cd}(e_z R) \rangle \quad (4)$$

where the colour indices a, b, c, d and the Dirac indices i, j, k, l are associated with vertices as in Fig. 1. The sum over Dirac indices is only from 1 to 2 since the heavy quark has a spin projection factor. These contributions can be evaluated for every choice of origin on a lattice which is translationally invariant. For the spin-dependent part with component p , we have

$$C_s^p(t) = \langle G_{ji}^{ba}(0, 0; 0, t) \sigma_{ij}^p U^{ab}(0) G_{lk}^{dc} \sigma_{kl}^p(e_z R, 0; e_z R, t) U^{cd}(e_z R) \rangle \quad (5)$$

For the ‘cross’ diagram the colour and spin sums are different, for example the contribution to C_I is given by

$$C_I(t) = -\langle G_{ki}^{da}(0, 0; e_z R, t) U^{cd}(e_z R) G_{ik}^{bc}(e_z R, 0; 0, t) U^{ab}(0) \rangle \quad (6)$$

where the negative sign comes from the Grassmannian nature of the fermions. For states symmetric under light quark interchange (eg. $I = 1$), then the sum of uncrossed and crossed diagram is needed, where the above minus sign is incorporated into the crossed diagram – this plays the rôle of the Pauli principle. For states antisymmetric under light quark interchange (eg. $I = 0$), the difference of uncrossed and crossed diagrams is needed.

3 Fermion formalism

The diagrams we need to evaluate are illustrated in Fig. 1. We need light quark propagators from more than one source – so the conventional approach

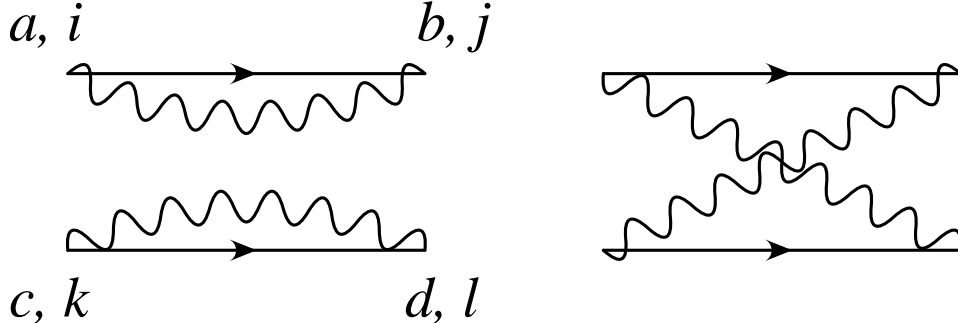


Figure 1: Diagrams showing the interaction between two \mathcal{B} mesons: the light quarks are shown as wiggly lines.

of inverting from a single source is impractical. One feasible way forward is to use a stochastic inversion method which allows the evaluation of quark propagators from any site to any other site. The stochastic method has already been shown to be more efficient than the conventional inversion from one source for mesons made of heavy-light quarks [16], and it does allow the flexibility to evaluate the required combinations of correlations readily. For this reason it allows a thorough study of this area.

Stochastic propagators [16, 15] are one technique to invert the fermionic matrix for the light quarks. They can be used in place of light quark propagators calculated with the usual deterministic algorithm. The stochastic inversion is based on the relation:

$$G_{ij} = \mathcal{M}_{ij}^{-1} = \frac{1}{Z} \int \mathcal{D}\phi (\mathcal{M}_{jk}\phi_k)^* \phi_i \exp(-\phi_i^* (\mathcal{M}^\dagger \mathcal{M})_{ij} \phi_j) \quad (7)$$

where, in our case, \mathcal{M} is the improved Wilson-Dirac fermionic operator and the indices i, j, k represent simultaneously the space-time coordinates, the spinor and colour indices. For every gauge configuration, an ensemble of independent fields ϕ_i (we use 24 following [16]) is generated with gaussian probability:

$$P[\phi] = \frac{1}{Z} \exp(-\phi_i^* (\mathcal{M}^\dagger \mathcal{M})_{ij} \phi_j) \quad (8)$$

All light propagators are computed as averages over the pseudo-fermionic

samples:

$$G_{ij} = \begin{cases} \langle (\mathcal{M}\phi)_j^* \phi_i \rangle \\ \text{or} \\ \gamma_5 \langle \phi_j^* (\mathcal{M}\phi)_i \rangle \gamma_5 \end{cases} \quad (9)$$

where the two expressions are related by $G_{ij} = \gamma_5 G_{ji}^\dagger \gamma_5$. Moreover, the maximal variance reduction method is applied in order to minimise the statistical noise [16]. The maximal variance reduction method involves dividing the lattice into two boxes ($0 < t < T/2$ and $T/2 < t < T$) and solving the equation of motion numerically within each box, keeping the pseudo-fermion field ϕ on the boundary fixed. According to the maximal reduction method, the fields which enter the correlation functions must be either the original fields ϕ or solutions of the equation of motion in disconnected regions. The stochastic propagator is therefore defined from each point in one box to every point in the other box or on the boundary. For more than one propagator from one box to the other, we need to use different stochastic samples for each. This is completely analogous to the technique used to discuss the Λ_b meson [16].

The numerical analysis used 24 stochastic samples on each of 60 quenched gauge configurations, generated [16] on a $12^3 \times 24$ lattice at $\beta = 5.7$, corresponding to $a^{-1} = 1.10$ GeV. With improved clover coefficient $C_{SW} = 1.57$, we use a value of $\kappa_1 = 0.14077$ which corresponds to a bare mass of the light quark around the strange mass and gives a pseudoscalar to vector mass ratio of $0.650(7)$. The chiral limit corresponds to $\kappa_c = 0.14351$ [18]. Error estimates come from bootstrap over the gauge configurations. We also used 20 quenched gauge configurations on a $16^3 \times 24$ lattice to check finite size effects with the same parameters as above. Allowing for the self-averaging effect of the larger spatial volume, this data set has similar weight to that at the smaller volume.

In smearing the hadronic interpolating operators, spatial fussed links are used. Following the prescription in [16, 17], the fussed links are defined iteratively as:

$$U_{\text{new}} = \mathcal{P} \left(f U_{\text{old}} + \sum_{i=1}^4 U_{\text{bend},i} \right) \quad (10)$$

where \mathcal{P} is a projector over $SU(3)$, and $U_{\text{bend},i}$ are the staples attached to the link in the spatial directions. Two iterations of fuzzing with $f = 2.5$ are

used and then the fuzzed links of length one are used. The fuzzed fermionic fields are defined following [17].

We employed two types of hadronic operator for the heavy-light mesons - local and fuzzed. Then for the initial state of two such mesons we have 4 basis states. If one restricts to the operators symmetric under interchange, then this leaves three operators, symbolically LL, LF+FL and FF. We then have a 3×3 matrix of correlations at time t between these states at initial and final time. From this we use a variational approach to extract the linear combination of operators which maximises the ground state contribution.

4 Results

Our results are for quenched lattices at $\beta = 5.7$ and we set the scale [16] from $(\text{string tension})^{1/2} = 0.44 \text{ GeV}$ (which implies $r_0 = 0.53 \text{ fm}$) using $r_0/a = 2.94$ to obtain $1/a = 1.10 \text{ GeV}$. This scale has systematic errors of at least 10% coming from the differences relative to experiment of different observables in the quenched approximation. There will also be lattice corrections which should be dominantly of order a^2 since we use clover improvement. Because of the similarity with the lattice spacing and GeV units, we present most of our results in lattice units with the understanding that they can be read as GeV to get an estimate of the physical units. Thus we are able to measure the strength of the interaction out to separations of $R \approx 8$ which will correspond roughly to 1.4 fm.

For the \mathcal{B} meson itself, needed to evaluate binding energies, we follow Ref. [16] and use either variational analyses or a fit to all correlations over a range of t -values. We find that there are substantial excited state contributions and that a good two-state fit is possible to our correlations from 60 gauge configurations for $5 \leq t$ with $\chi^2/\text{dof} = 2.4/(15 - 6)$ yielding $m_B = 0.876(6)$. This can be contrasted with the value of 0.875(6) obtained in Ref. [16] from a fit for $5 \leq t$ to a larger variational basis from 20 gauge configurations. For a variational study, we determine the basis from using t of 3 and 4 and then follow the effective mass in that basis to larger t to look for a plateau which we find by t values of 6 and 7 - see Table 2. This gives similar results to the fit approach.

For a study of the $\mathcal{B}\mathcal{B}$ system, one approach would be to use the variational basis found in the \mathcal{B} meson study for each of the two \mathcal{B} mesons. This will certainly be a good approach at large R when any interaction between the two \mathcal{B} mesons will be very small. We shall use this basis to give an overview of the relative size of different contributions to the interaction.

A more sophisticated approach would be to make a new variational study of the $\mathcal{B}\mathcal{B}$ system itself. The spatially-symmetric sector is described by a 3×3 matrix as discussed above. We find in practice that this $\mathcal{B}\mathcal{B}$ optimal basis gives very similar results to using the \mathcal{B} meson basis for each \mathcal{B} meson.

Given that a combined fit was found to be the method of choice for the \mathcal{B} meson study [16], we should also investigate fits to the $\mathcal{B}\mathcal{B}$ correlations. One problem is that if the \mathcal{B} is described by two states, then $\mathcal{B}\mathcal{B}$ will require three energy eigenstates ($\mathcal{B}\mathcal{B}$, $\mathcal{B}'\mathcal{B}$, and $\mathcal{B}'\mathcal{B}'$). This increase in parameters makes the fit less stable.

In each case, we can use a bootstrap method to study the binding energy by using the same subsets of gauges for the $\mathcal{B}\mathcal{B}$ and \mathcal{B} studies.

For this study, we use on-axis separations $R = 0, 1, \dots, 5$ for spatial size 12^3 and $R = 0, 1, \dots, 8$ for 16^3 . We also measured the correlation for the off-axis separation of $R = (\pm 1, \pm 1, 0)$ in both cases.

Overview of results. We first discuss our results from 12^3 spatial lattices in terms of the ratios of contributions to the uncrossed diagram for spin average (C_I), taking the \mathcal{B} meson basis discussed above. For the $\mathcal{B}\mathcal{B}$ correlator in this basis divided by the square of the \mathcal{B} correlator in the same basis, we find the results given in Fig. 2. This shows that, for $R > 2$, we find this ratio to be consistent with constant versus t . This constancy implies that there would be no binding energy for this correlation within the errors. The fact that the ratio is larger than one can be explained as a consequence of the fluctuation with spatial location and gauge configuration of the \mathcal{B} meson correlator and the property that $\langle c^2 \rangle > \langle c \rangle^2$ for a fluctuating quantity c . The relatively large statistical error on the signal of interest, the departure of the ratio in Fig. 2 from 1.0, is consistent with the observation that disconnected quark diagrams (as this is) are noisier in lattice simulations than connected diagrams (such as the crossed diagram).

The ratio of the spin-averaged $\mathcal{B}\mathcal{B}$ correlation from the cross diagram to that from the uncrossed diagram is shown in Fig. 3. The ratio is seen to increase

with t and to decrease with R ($R = 0$ is anomalous). This t -dependence implies an interaction, and we find it to decrease in relative strength with increasing R .

The uncrossed spin flip correlation (C_s averaged over x , y and z) is fairly small as shown in Fig. 4 and has big errors. The dominant contribution to the spin-flip comes from the cross diagram as illustrated in Fig. 5. In both cases, the spin-flip correlation is poorly determined at larger R . We shall discuss these contributions in terms of particle exchange later.

We find that the uncrossed diagram mainly contributes to the spin average, while the crossed diagram contributes a comparable amount to the spin-flip and spin average. This is easy to understand since crossing the quarks will cause the spin average component ($s_1s_2 \rightarrow s_3s_4$ of $+- \rightarrow +-$) to become $+- \rightarrow -+$ which is spin flip. We also looked at the tensor interaction ($2C_s(z) - C_s(x) - C_s(y)$) but found a small and poorly determined signal.

In the analysis presented above, the \mathcal{B} meson ground state has been extracted by using the variational basis found from a study of a single \mathcal{B} meson. It is not feasible to construct a pure two meson state on a lattice in Euclidean time since asymptotic states cannot be constructed. Rather, one can only construct a state with given quantum number and then extract the energy eigenvalues. Nevertheless, a qualitative understanding can be obtained, as above, by constructing approximations to the two meson state and exploring their correlations.

For example if we find that the ratio $C_s/C_I \approx C + Dt$, and if the combinations $C_I + f_1C_s$ and $C_I + f_2C_s$ correspond to two given sets of quantum numbers 1, 2 in the $\mathcal{B}\mathcal{B}$ channel, then the mass difference which is obtained from the t -dependence of these correlators at large t satisfies

$$E_1 - E_2 = \frac{d}{dt} \log \frac{C_I + f_2C_s}{C_I + f_1C_s} \approx \frac{d}{dt} (f_2 - f_1)(C + Dt) \approx (f_2 - f_1)D \quad (11)$$

if C_s/C_I is small. Thus a linear dependence of the ratio is expected and can be related to the energy difference as shown. We do indeed see evidence for such linear behaviours of ratios in the figures just discussed. This linear dependence of the spin-flip correlation on t can also be related theoretically to a meson exchange interpretation, for example, and we discuss this later.

Energy Levels. A study of correlations between lattice operators at increasing

t allows an analysis of energy levels. Thus by taking the appropriate combination of crossed and spin-flip contributions, the energy of $\mathcal{B}\mathcal{B}$ states with different quantum numbers can be studied. Because the binding energies are found to be quite small, we have presented the foregoing discussion to show the quality of our lattice data.

We present the energies for isospin 0 and 1 light quarks for the triplet and singlet spin combinations, using a 3×3 variational basis from t of 4 and 3 to obtain the optimum combination for the $\mathcal{B}\mathcal{B}$ ground state. Here we use $C_I + C_s$ correlation for the triplet states with C_s the average over orientation which is appropriate for an S -wave bound state and $C_I - 3C_s$ for the singlet states. The energies evaluated on a lattice include a contribution from the self-energy of the static source which is unphysical. Thus only energy differences have a physical significance and hence we concentrate especially on the binding energies – the difference of $\mathcal{B}\mathcal{B}$ energy from twice the \mathcal{B} energy. In the special case of $R = 0$, we show the actual lattice energy values in Table 2 to allow us to discuss the extrapolation to large t needed to extract the ground state. Other results are given in Table 3 for the case of $R = 3$ and in Figs. 6 to 9. We show the results from both 12^3 and 16^3 spatial lattices with the same parameters in order to explore finite size effects. Within errors, we do not see significant differences in the results between spatial sizes of $L = 12$ and 16, which is not unexpected since a study of the \mathcal{B} meson using $L = 8$ and 12 found [16] agreement for the energies of the ground state mesons and a relatively localised Bethe-Saltpeter wave function.

The situation at $R = 0$ is special because the two static b quarks can be classified under their combined colour into either an anti-triplet or a sextet. The former case is just that which applies to baryons with one static quark and these are expected to be the lightest states. Thus the $\mathcal{B}\mathcal{B}$ spectrum at $R = 0$ is expected to reproduce these baryonic levels. As shown in Table 2, we find excellent agreement with the masses of baryonic states with one static quark which have been obtained on the lattice previously [16]. This is a useful cross check of our procedures for obtaining energy levels. Thus we find that the Λ_b (with light quarks of $I = 0$ and in a spin singlet) is the lightest state. Combining with the \mathcal{B} meson mass then gives an estimate of the binding energies at $R = 0$ which will agree well with those we obtain here – namely around 400 MeV for the $I_q, S_q = (0, 0)$ state. We are also able to explore the energies of states with $R = 0$ having the opposite symmetry

Table 2: Effective masses for \mathcal{B} and for $\mathcal{B}\mathcal{B}$ at $R=0$

I_q	S_q	L	E_{eff}			ref[16]
			t -ratio:	5/4	6/5	
\mathcal{B}						
1/2	1/2	12	0.911(3)	0.893(3)	0.873(6)	0.875(6)
$\mathcal{B}\mathcal{B}$						
1	1	12	1.620(9)	1.516(12)	1.558(32)	1.514(52)
		16	1.589(10)	1.539(18)	1.476(35)	
0	0	12	1.472(18)	1.412(29)	1.301(63)	1.435(37)
		16	1.458(17)	1.420(31)	1.348(48)	
1	0	12	1.864(22)	1.806(44)	1.629(111)	
		16	1.915(19)	1.882(50)	1.827(130)	
0	1	12	1.911(19)	1.852(36)	1.722(109)	
		16	1.860(18)	1.865(43)	2.886(134)	

– so corresponding to the sextet of colour which is symmetric (rather than the anti-triplet which is antisymmetric). We find these states to lie higher in mass than the anti-triplet states by about 0.3 in lattice units as shown in Table 2 and to be unbound.

Unlike on the lattice, where for static quarks, the binding energy at $R = 0$ can be obtained by taking the difference of the lattice baryon mass with twice the lattice \mathcal{B} mass, in the continuum, in the heavy quark limit, one would expect that the binding of the $\mathcal{B}\mathcal{B}$ system at $R = 0$ for light quark flavour of $I = 0$ is given by $2(M_B - m_b) - (M_{\Lambda_b} - m_b)$ where m_b is the b -quark mass.

Since we find that the variational method gives a plateau from t -values of 5 and 6, as shown in Table 2, we expect that that would be a good criterion to use for $R > 0$.

However, for the \mathcal{B} meson case itself, it is found that our variational method does not achieve a plateau value for the effective mass until a t -ratio of 7 to 6 as shown in Table 2. At these large t -values, the $\mathcal{B}\mathcal{B}$ signal is very noisy. Since the same operators are used for the $\mathcal{B}\mathcal{B}$ case as for the \mathcal{B} meson alone, it is feasible that excited state contributions are dealt with similarly

Table 3: Binding energies for $\mathcal{B}\mathcal{B}$ at $R=3a$

I_q	S_q	L	$E(\mathcal{B}\mathcal{B}) - 2E(\mathcal{B})$		
			t -ratio:		
			5/4	6/5	7/6
1	1	12	0.027(5)	0.019(13)	0.012(32)
		16	0.024(4)	0.023(12)	0.005(41)
0	0	12	0.035(10)	0.050(30)	0.021(90)
		16	-0.013(13)	0.034(32)	-0.000(85)
1	0	12	-0.002(10)	-0.077(23)	0.040(72)
		16	-0.030(10)	-0.003(22)	0.069(92)
0	1	12	-0.029(6)	-0.040(10)	-0.061(38)
		16	-0.021(7)	-0.038(12)	-0.019(42)

in each case, particularly for $R > 0$ where the binding energy is found to be very small. Thus it makes sense to study the difference (the binding energy) obtained from the $\mathcal{B}\mathcal{B}$ effective mass at a given t -ratio and twice the \mathcal{B} meson effective mass at the same t -ratio. This is plotted in Figs. 6 to 9 from the ratio of correlations at t -values of 5 and 6.

To explore the consistency of the binding energy obtained in this way, we show in Table 3 at $R = 3$ the variational effective mass differences from different t -values. This leads us to conclude that the variational effective mass values for the binding energy are consistent with being constant within errors from t -values of 5/4, the excited state contamination being smaller than for the total energies. For extra safety in extracting the ground state, we shall use the effective mass from the t -values of 6/5, as stated above.

As a cross check of this procedure, we find that the binding energy is consistent with zero within errors at large R , namely $R \geq 5$.

As one goes to nonzero R , the level ordering found at $R = 0$ would be expected to be retained if the dominant dynamical configuration was that the two heavy quarks combine to an anti-triplet. We illustrate the binding energies for these states analogous to the Λ_b in Fig. 7 and the Σ_b in Fig. 6. We see the level ordering to persist for the smallest values of R , the binding disappearing at $R \approx 0.2$ fm for the Σ_b -like state and at $R \approx 0.3$ fm for the

Λ_b analogue. The binding for the other pair of states is shown in Figs. 8 and 9. Here we see that the $I_q, S_q=(0,1)$ state shows a statistically significant binding of 40 MeV at $R \approx 0.5$ fm. The situation for the $I_q, S_q=(1,0)$ state is less clear, since the statistical fluctuation is larger, but it is consistent with a similar interpretation. Note that pion exchange in the cross diagram will act to make the $I_q, S_q = (1,0)$ and $(0,1)$ states lightest at large R as we discuss in more detail later.

5 Discussion

Bound states. We find binding at small R for $I_q, S_q=(0,0)$ and $(1,1)$ and binding at moderate R (circa 0.5 fm) for $(1,0)$ and $(0,1)$. For very heavy quarks, this will imply binding of the $\mathcal{B}\mathcal{B}$ molecules with these quantum numbers and $L = 0$. For the physically relevant case of b quarks of around 5 GeV, the kinetic energy will not be negligible and the binding energy of the $\mathcal{B}\mathcal{B}$ molecular states is less clear cut. One way to estimate the kinetic energy for the $\mathcal{B}\mathcal{B}$ case with reduced mass circa 2.5 GeV is to use analytic approximations to the potentials we find. For example the $I_q, S_q=(0,0)$ case shows a deep binding at $R = 0$ which we can approximate as a Coulomb potential of $-0.1/R$ in GeV units. This will give a di-meson binding energy of only 10 MeV. For the other interesting case, $I_q, S_q=(0,1)$, a harmonic oscillator potential in the radial coordinate of form $-0.04[1 - (r - 3)^2/4]$ in GeV units leads to a kinetic energy which completely cancels the potential energy minimum, leaving zero binding. This harmonic oscillator approximation lies above our estimate of the potential, so again we expect weak binding of the di-meson system.

Because of these very small values for the di-meson binding energies, we need to retain corrections to the heavy quark approximation to make more definite predictions, since these corrections are known to be of magnitude 46 MeV for the \mathcal{B} system. It will also be necessary to extrapolate our light quark mass from strange to the lighter u, d values to make more definite predictions about the binding of B mesons. This is especially necessary for light meson exchange contributions, which discuss subsequently.

A model for static four-quark systems is extended and fitted to our binding energies in Ref. [19]. As in the static case, the results point out the inad-

equacy of a simple two-body potential approach for describing multi-quark systems. Inclusion of a multi-quark interaction term interpolating between strong and weak coupling regimes enables reproduction of the lattice data.

One meson exchange. The interaction responsible for the binding energy in the $\mathcal{B}\mathcal{B}$ system can be discussed in terms of meson exchange. One simple criterion is that $\mathcal{B}\mathcal{B} \rightarrow \mathcal{B}\mathcal{B}$ only allows natural parity exchange (such as vector meson exchange) while $\mathcal{B}\mathcal{B}^* \rightarrow \mathcal{B}^*\mathcal{B}$ has an unnatural parity exchange component as well. Here natural means that the exchanged mesons have parity $(-1)^J$. This can be explored by viewing the diagrams of Fig. 1 as representing a (spatially non-local) meson creation at $z = z_1$ and then annihilation at $z_2 = z_1 + R$. The quantum numbers of the mesons propagating in the z -direction then can be determined from the Dirac structure of the effective creation operator. So for C_I ($\mathcal{B}\mathcal{B} \rightarrow \mathcal{B}\mathcal{B}$), we have scalar and vector mesons allowed (natural parity exchanges), while for $C_s(z)$, we have pseudoscalar and axial (unnatural parity exchanges), while for $C_s(x)$ and $C_s(y)$, both axial and vector are allowed. From this analysis it follows that at large R , the correlations at fixed t behave as $\exp(-MR)$ with M the mass corresponding to the lightest meson exchange allowed. For our lattice parameters, these will be the pseudoscalar meson, mass 0.529(2), for $C_s(z)$ and vector meson, mass 0.815(5), for C_I .

Meson exchange contributes to the uncrossed diagram with flavour singlet exchange only while the crossed diagram has both flavour singlet and non-singlet mesons exchanged. In the quenched approximation, the flavour singlet and flavour non-singlet mesons are degenerate. However, in full QCD, the flavour singlet mass is modified by quark loop effects which are not present in the quenched case. These effects are responsible for the η, η' mass splitting, for example. Thus to make the cleanest comparison with meson exchange, it is appropriate to use the flavour non-singlet mesons (π, ρ etc) which contribute only to the crossed diagram. Furthermore, our determinations of the contributions from the uncrossed diagram are considerably more noisy, so this comparison with the crossed diagram alone will be a tighter test.

Then, as shown in Fig. 10, we see evidence for an exponential decrease of the interaction with increasing separation R with a mass exponent consistent with that expected, namely, vector for C_I and pseudoscalar for $C_s(z)$. This agreement with the nature of the lightest meson exchange is a confirmation that the arguments given above apply at modest R values. Since the lattice

operator which creates the meson is not at zero momentum, we expect non-exponential contributions to yield the expression $(1/R) \exp(-MR)$ where we have assumed that a sum over the t -direction is taken (so t is large: here we need $t > (2R/M)^{1/2}$ which is satisfied in our case). This expression is just the conventional Yukawa potential.

It is possible to go further, since lattice estimates for the $B^*B\pi$ coupling are available [22] from a study of the axial matrix element between B and B^* . Indeed, as well as the coupling itself, this lattice study also measures the form factor – the spatial distribution of the coupling – which is found to be quite localised. So we are able to evaluate the magnitude of the pion exchange contribution using the lattice pion – so affording a direct comparison.

Now consider the interaction potential for $B^*B \rightarrow B^*B$ with B^* spin polarisation in the z -direction, which has a one pion exchange component at large R ,

$$V(R) = \vec{\tau}_1 \cdot \vec{\tau}_2 \frac{g^2 M^2}{4\pi f^2} \frac{e^{-MR}}{R} \quad (12)$$

where g/f is the pion coupling to quarks [5] and we use the value determined from the lattice [22] of $g = 0.42(8)$ and where f is the pion decay constant (132 MeV). Because we wish to compare with our lattice results with heavier light quarks, we use the lattice pion mass ($Ma = 0.53$).

Then to compare with our best determined quantity, the ratio of the crossed diagram contribution to $C_s(z)$ to the uncrossed contribution to C_I , we assume that the ratio is small so that a linear t -dependence is appropriate, as indeed is compatible with our lattice results in Fig. 5. This implies that

$$\frac{C_s^X(z)}{C_I^D} = \frac{t}{2} \frac{g^2 M^2}{4\pi f^2} \frac{e^{-MR}}{R} \quad (13)$$

and we plot this for $t = 5$ in Fig. 10, using the parameters discussed above.

The agreement is excellent – better than should be expected given that $t = 5$ is used and the signal is only well measured for $R < 5$. In particular, non-leading contributions will be of order $1/(MR)$ which is relatively large, namely $1/(MR) = 0.47$ at $R = 4$ for our lattice pion exchange, also note that some non-relativistic treatments of pion exchange have an explicit non-leading correction factor given by $1 + 3/(MR)$. This implies that we should not take our estimate of the magnitude of one pion exchange as more than

a rough guide at the R -values we are able to measure. Furthermore, for consistency, we should use the lattice determination of f for our lattice pion mass (which corresponds to quarks with the strange mass), hence f will be somewhat larger (by a factor of around $f_K^2/f_\pi^2 = 1.4$). What our comparison does show, however, is that the pion exchange contribution to the binding can be identified reliably for $R \approx 0.5$ fm. This allows the realistic pion mass to be used to give predictions for the physical case with more confidence because of the agreement we find for pions heavier than the physical case.

Note that the pion exchange contribution is to $C_s(z)$ only which will contribute a large tensor interaction. Thus, much as for the case of deuterium, this is likely to be responsible for mixing between S and D wave components in the di-meson bound states. Thus implications for bound states are not straightforward.

In deuson models, the analysis of the pion exchange contribution to the potential makes meson-antimeson states in most cases significantly more bound than meson-meson systems. The possibility is raised in Ref. [5] that B^*B^* states bound by pion exchange may exist. In such models, however, the small R behaviour of the potential is not reliable. As discussed above, the most fruitful way to use our results would be to take our non-perturbative measurement of the binding energy at small R and to modify our meson exchange component at larger R to have the lighter pion mass which is physically relevant.

6 Conclusions

We study the $\mathcal{B}\mathcal{B}$ system at fixed separation R using static b -quarks. We present evidence for deep binding at small R with the light quark configuration similar to that in the Λ_b and Σ_b baryons – so that the heavy quarks are in a colour-triplet di-quark state (and the light quarks have $I_q, S_q=(0,0)$ and $(1,1)$ respectively). This binding energy is 400 - 200 MeV at $R = 0$ but is very short-ranged. This binding is essentially a gluonic effect and is rather insensitive to the light quark mass, as shown by studies of the static baryons with varying light quark masses [16]. At larger R , around 0.5 fm, we see evidence for weak binding when the light quarks are in the $I_q, S_q=(0,1)$ and $(1,0)$ states. This can be related to meson exchange and we find evidence of

an interaction in the spin-dependent quark-exchange (cross) diagram which is compatible with the theoretical contribution from pion exchange in our study. Using lighter, and hence more physical, light quark masses, this effect will be modified in a predictable way, although further lattice study is needed with light quark masses below those we use (namely strange) to confirm this. Corrections also need to be evaluated to the heavy quark limit for applications to realistic b -quarks and we need to use smaller lattice spacings so reaching closer to the continuum limit, together with gauge configurations which have the contributions from sea quarks included.

Our results show that it is plausible that exotic $bb\bar{q}\bar{q}$ di-mesons exist as states stable under strong interactions. With the future lattice developments described above, it will be possible to give a definite answer from first principles in QCD whether this is so.

7 Acknowledgement

We thank T. Barnes, A.M. Green and E. Swanson for discussions and the Helsinki Institute of Physics for hospitality. We acknowledge the support from PPARC under grants GR/L22744 and GR/L55056 and from the HPCI grant GR/K41663.

References

- [1] M. B. Voloshin and L. B. Okun, *Pisma Zh. Eksp. Teor. Fiz.* **23**, 369 (1976).
- [2] R. L. Jaffe, *Phys. Rev.* **D15**, 267 (1976); C. W. Wong and K. F. Liu, *Phys. Rev.* **D21**, 2039 (1980).
- [3] F. Gutbrod, G. Kramer and C. Rumpf, *Zeit. Phys.* **C1**, 391 (1979).
- [4] C. Caso *et. al.*, *Review of Particle Physics*, *Eur. Phys. J.* **C3**, 1 (1998).
- [5] N. A. Törnqvist, *Phys. Rev. Lett.* **67**, 556 (1991); *Z. Phys.* **C61**, 525 (1994), [hep-ph/9310247](https://arxiv.org/abs/hep-ph/9310247).

- [6] M. M. Boyce, *String inspired QCD and E(6) models*, Ph.D. thesis, Carleton University, 1996, [hep-ph/9609433](#).
- [7] H. J. Lipkin, Phys. Lett. **B172**, 242 (1986).
- [8] S. Zouzou, B. Silvestre-Brac, C. Gignoux and J.-M. Richard, Z. Phys. **C30**, 457 (1986); J.-M. Richard, *Hadrons with two heavy quarks*, Proc. Conf. on future of high sensitivity charm experiments, Batavia (1994), [hep-ph/9407224](#).
- [9] A. M. Green, J. Lukkarinen, P. Pennanen and C. Michael, Phys. Rev. **D53**, 261 (1996), [hep-lat/9508002](#).
- [10] P. Pennanen, Phys. Rev. **D55**, 3958 (1997), [hep-lat/9608147](#); A. M. Green and P. Pennanen, Phys. Lett. **B426**, 243 (1998), HIP-1997-55 / TH, [hep-lat/9709124](#); *ibid.* Phys. Rev. **C57**, 3384 [hep-lat/9804003](#).
- [11] P. Pennanen, A. M. Green and C. Michael, Phys. Rev. **D59**, 014504-1 (1999), [hep-lat/9804004](#).
- [12] D. Richards, D. Sinclair and D. Sivers, Phys. Rev. **D42**, 3191 (1990).
- [13] C. Stewart and R. Koniuk, Phys. Rev. **D57**, 5581 (1998), [hep-lat/9803003](#).
- [14] A. Mihaly, H. R. Fiebig, H. Markum and K. Rabitsch, Phys. Rev. **D55**, 3077 (1997); H. R. Fiebig, H. Markum, A. Mihaly, K. Rabitsch and R. M. Woloshyn, Nucl. Phys. Proc. Suppl. **63**, 188 (1998), [hep-lat/9709152](#).
- [15] G. M. de Divitiis, R. Frezzotti, M. Masetti and R. Petronzio, Phys. Lett. **B382**, 393–397 (1996), [hep-lat/9603020](#).
- [16] UKQCD Collaboration, C. Michael and J. Peisa, Phys. Rev. **D58**, 034506-1 (1998), [hep-lat/9802015](#).
- [17] UKQCD Collaboration, P. Lacock, A. McKerrell, C. Michael, I.M. Stopher, P.W. Stephenson, Phys. Rev. **D51**, 6403 (1995), [hep-lat/9412079](#).

- [18] UKQCD Collaboration, H. Shanahan et al., Phys. Rev. **D55**, 1548 (1997), [hep-lat/9608063](#).
- [19] A. M. Green, J. Koponen and P. Pennanen, in progress.
- [20] UKQCD Collaboration: C.R. Allton, S.P. Booth, K.C. Bowler, M. Foster, J. Garden, A.C. Irving, R.D. Kenway, C. Michael, J. Peisa, S.M. Pickles, J.C. Sexton, Z. Sroczynski, M. Talevi, H. Wittig, OUTP-98-53-P, [hep-lat/9808016](#).
- [21] P. Pennanen, A.M. Green, C. Michael, Proceedings of LATTICE98, Boulder, CO (1998), [hep-lat/9809035](#); C. Michael, Proceedings of Confinement III, Newport News, VA (1998), [hep-ph/9809211](#).
- [22] UKQCD Collaboration, G. M. de Divitiis et al., J. High Energy Phys. 9810, 10, [hep-ph/9807032](#).

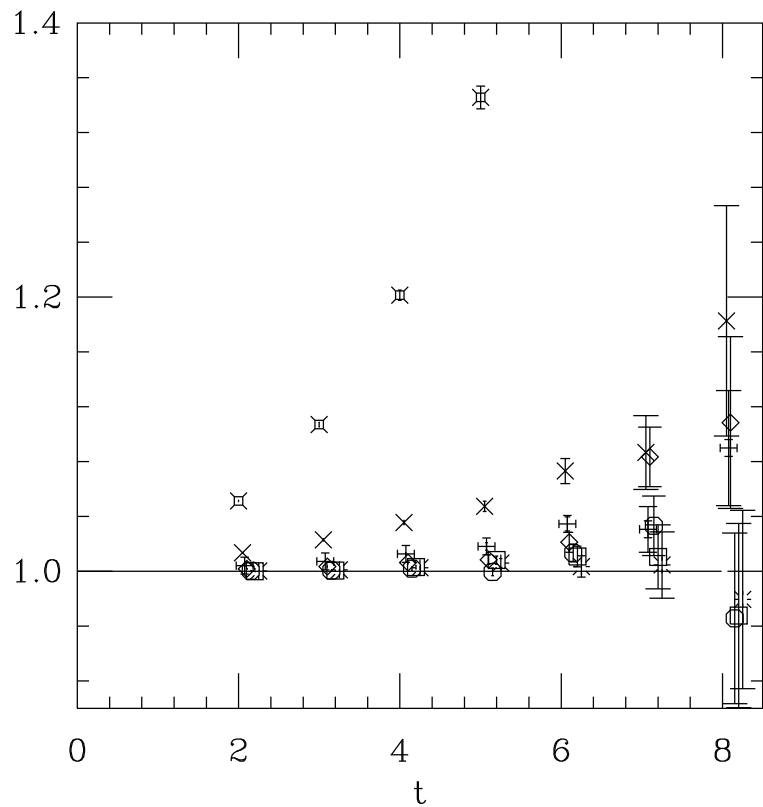


Figure 2: Results for ratio of uncrossed diagram for the spin average (corresponding to C_I) for two \mathcal{B} mesons divided by the product of two \mathcal{B} meson correlators, versus t . The separation R is 0 (fancy square), 1 (\times), $(1,1,0)$ (fancy plus), 2 (diamond), 3(octagon), 4 (square) and 5 (*) in lattice units.

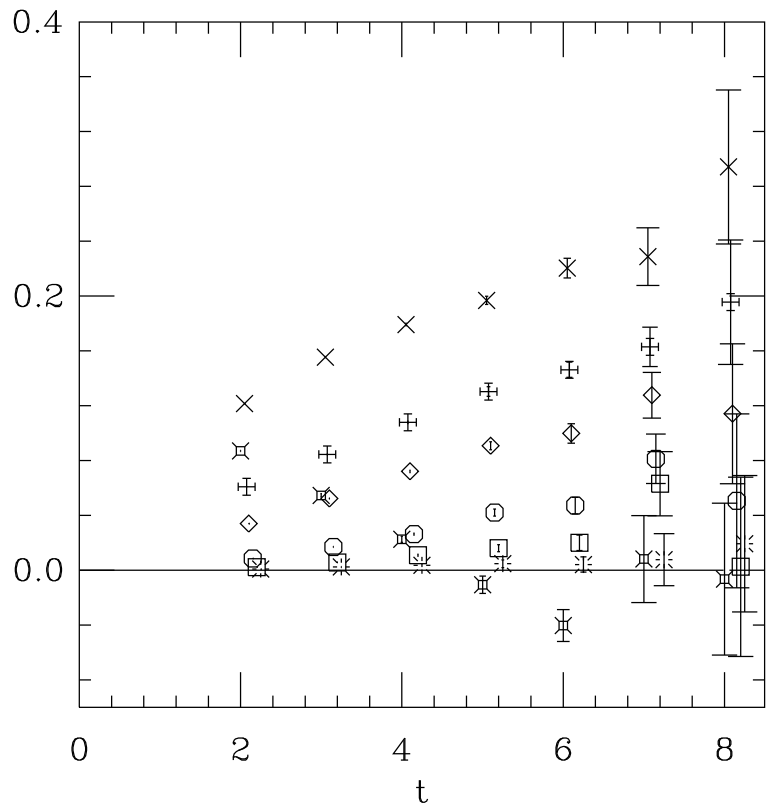


Figure 3: Results for ratio of cross diagram to uncrossed diagram for the spin average (corresponding to C_I) for two \mathcal{B} mesons versus t . The separation R is 0 (fancy square), 1 (\times), $(1,1,0)$ (fancy plus), 2 (diamond), 3(octagon), 4 (square) and 5 (*) in lattice units.

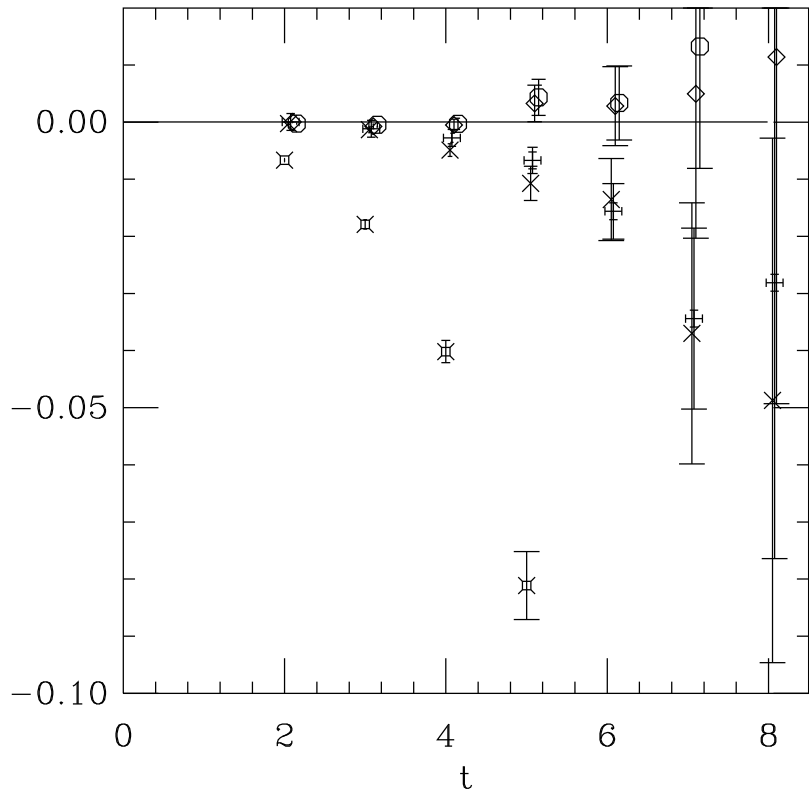


Figure 4: Results for ratio of spinflip to spin average (corresponding to C_s/C_I) for the uncrossed diagram with two \mathcal{B} mesons versus t . The separation R is 0 (fancy square), 1 (\times), $(1,1,0)$ (fancy plus), 2 (diamond) and 3(octagon) in lattice units.

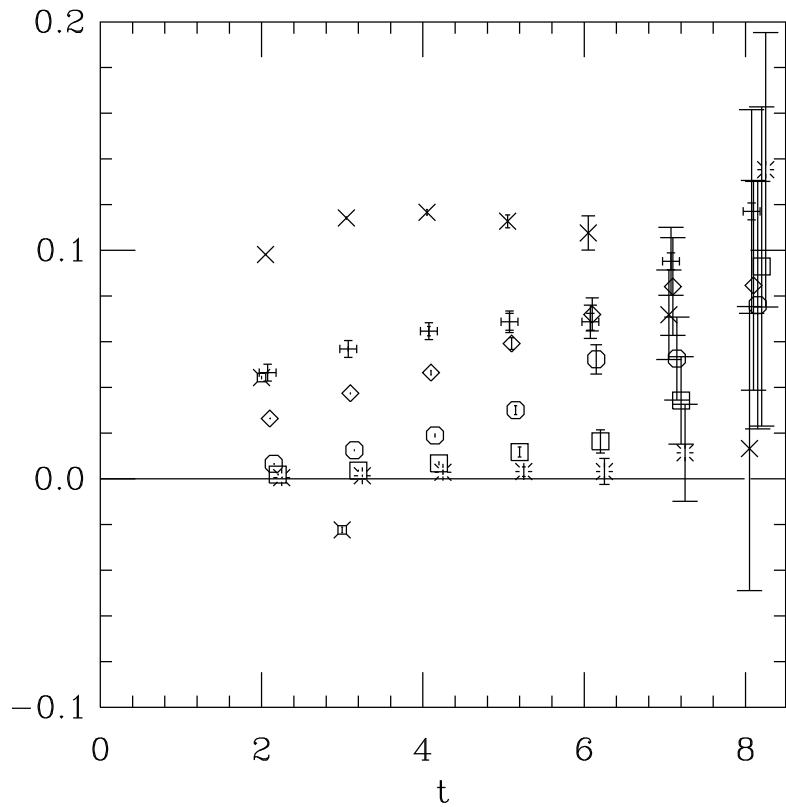


Figure 5: Results for ratio of spinflip cross diagram to spin average uncrossed diagram (corresponding to C_s/C_I) for two \mathcal{B} mesons versus t . The separation R is 0 (fancy square), 1 (\times), (1,1,0) (fancy plus), 2 (diamond), 3(octagon), 4 (square) and 5 (*) in lattice units.

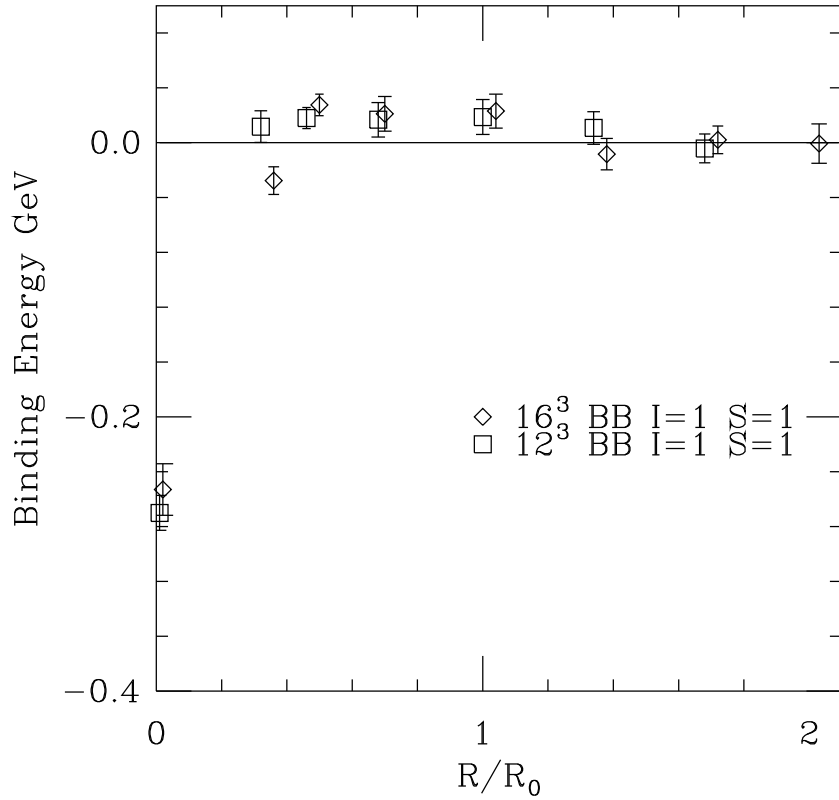


Figure 6: Results for the binding energy between two \mathcal{B} mesons with light quarks in $(I_q, S_q)=(1,1)$ at separation R in units of $R_0 \approx 0.5\text{fm}$. The light quark mass used corresponds to strange quarks. Results from variational method using basis from t 4:3 and effective mass in that basis from t 6:5. Results at different spatial lattice sizes are displaced in R for legibility.

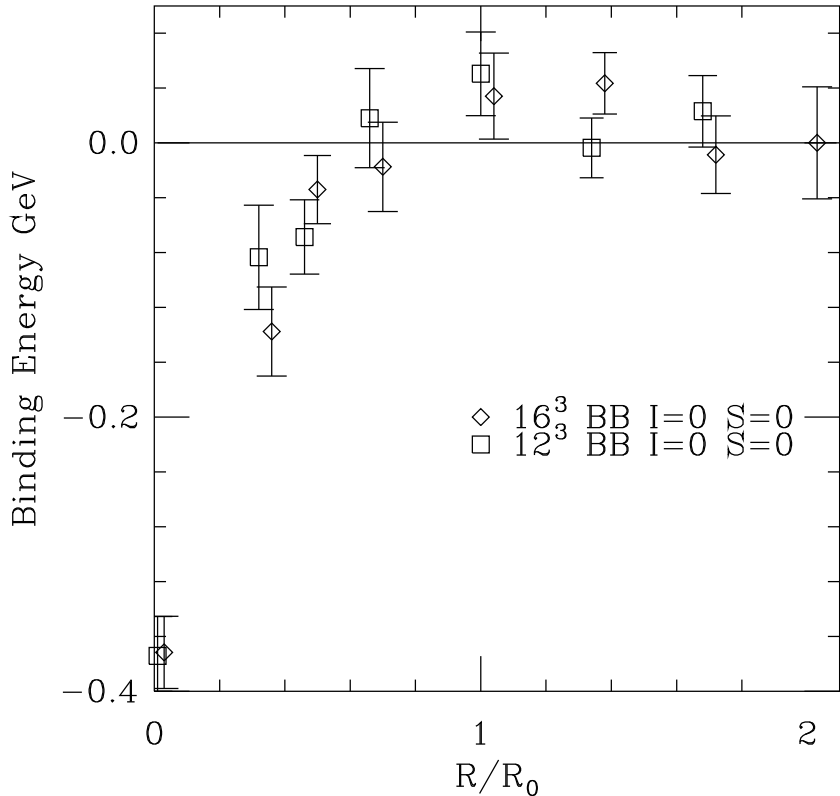


Figure 7: Results for the binding energy between two \mathcal{B} mesons with light quarks in $(I_q, S_q) = (0,0)$ at separation R in units of $R_0 \approx 0.5\text{fm}$. The light quark mass used corresponds to strange quarks. Results from variational method using basis from $t\ 4:3$ and effective mass in that basis from $t\ 6:5$.

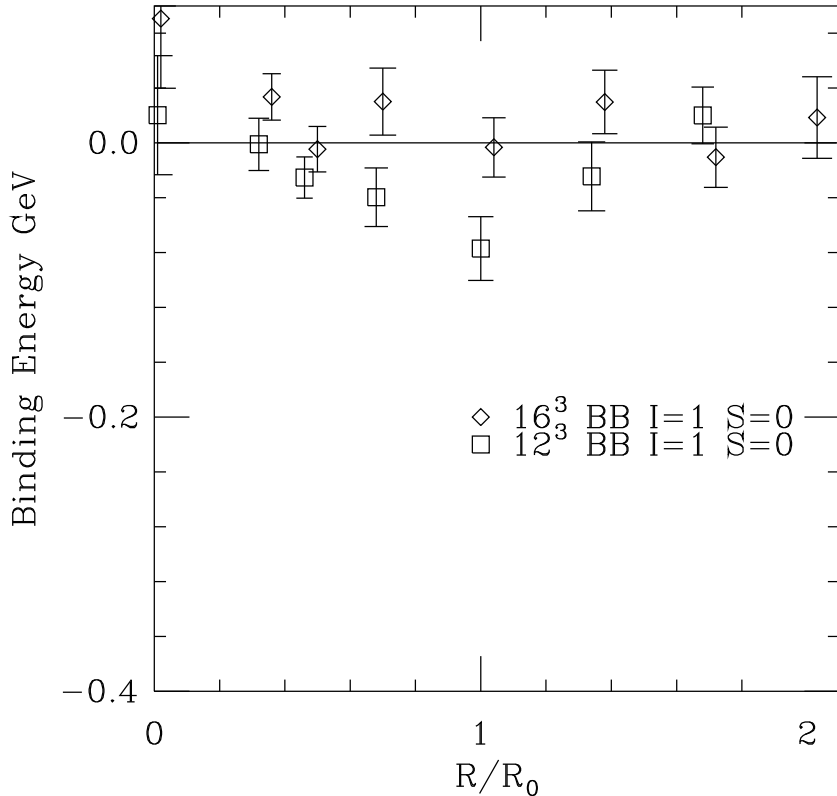


Figure 8: Results for the binding energy between two \mathcal{B} mesons with light quarks in $(I_q, S_q) = (1, 0)$ at separation R in units of $R_0 \approx 0.5\text{fm}$. The light quark mass used corresponds to strange quarks. Results from variational method using basis from $t\ 4:3$ and effective mass in that basis from $t\ 6:5$.

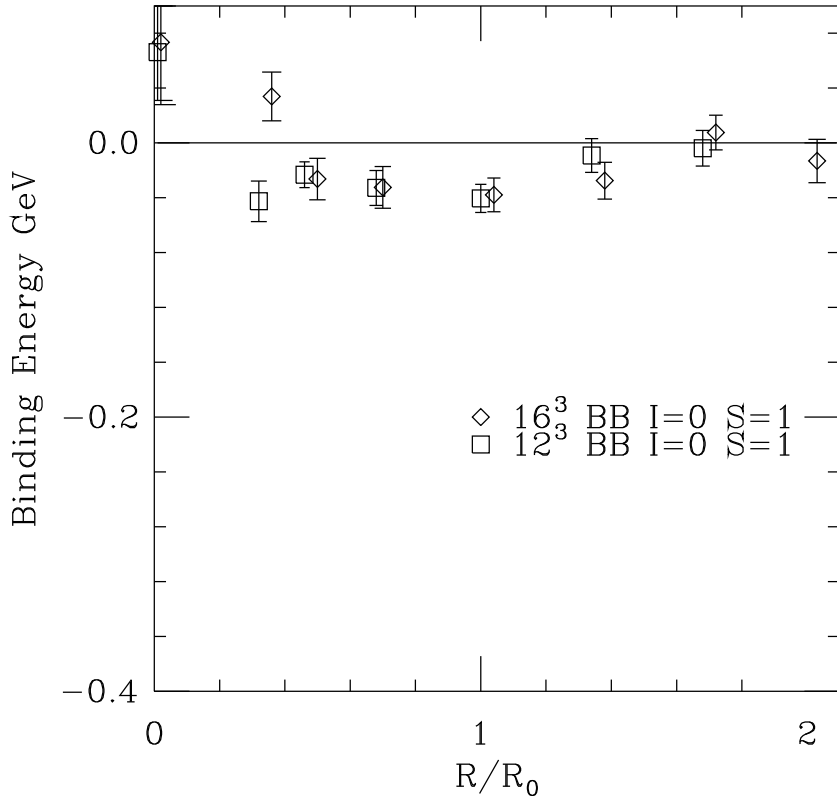


Figure 9: Results for the binding energy between two \mathcal{B} mesons with light quarks in $(I_q, S_q) = (0,1)$ at separation R in units of $R_0 \approx 0.5\text{fm}$. The light quark mass used corresponds to strange quarks. Results from variational method using basis from $t\ 4:3$ and effective mass in that basis from $t\ 6:5$.

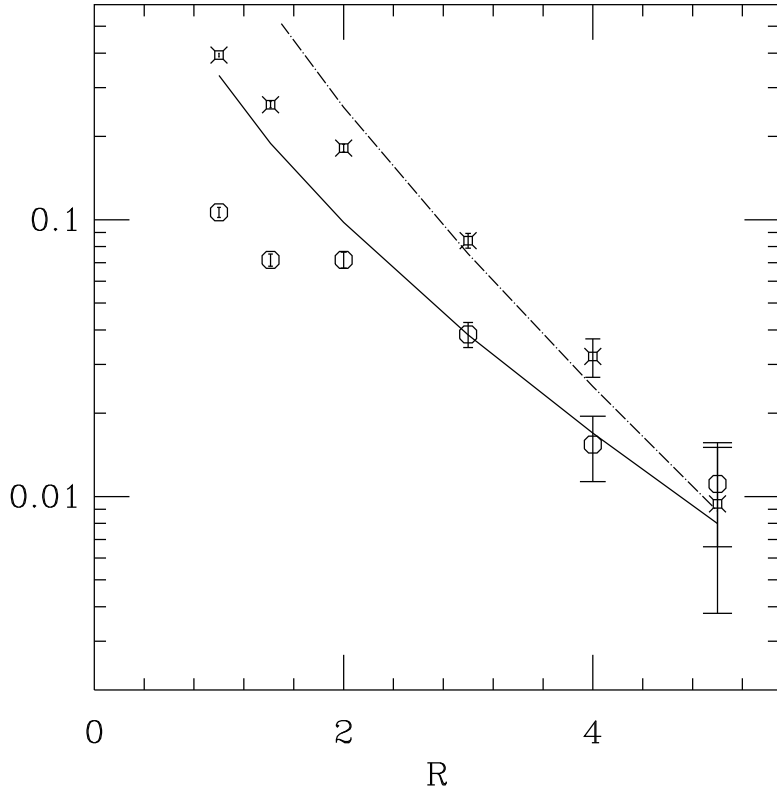


Figure 10: The ratio of the crossed-diagram contributions to the spin averaged uncrossed contribution for the $\mathcal{B}\mathcal{B}$ correlation at $t=5$. Shown are the crossed diagram correlation for the spin average ($\mathcal{B}\mathcal{B} \rightarrow \mathcal{B}\mathcal{B}$, C_I , multiplied by two for clarity of presentation, fancy squares) and the spin-flip ($\mathcal{B}\mathcal{B}^* \rightarrow \mathcal{B}^*\mathcal{B}$, $C_s(z)$, octagons). The meson exchange expressions, $\exp(-MR)/R$, are compared with these results for $C_s(z)$ (using pion exchange with $M = 0.529$, continuous line) and for C_I (rho exchange with $M = 0.815$, dotted). Note that the pion exchange expression is normalised as described in the text, whereas the rho exchange contribution has an ad hoc normalisation.